A One-Step Solution Technique for Elastic-Plastic Self-Similar Problems

Ståhle, P.

Published in:
International Journal of Fracture

DOI:
10.1007/BF00034575

1986

Document Version:
Peer reviewed version (aka post-print)

International Journal of Fracture 30 (1986) 5–12

A one-step solution technique for elastic-plastic self-similar problems

P. STÅHLE

Division of Solid Mechanics, Lund Institute of Technology, Lund, Sweden

(Received 18 March 1985; in revised form 18 September 1985)

Abstract

At self-similarity the strain history is implicit in and deducible from the strain field at each instance of the loading process. This fact is taken advantage of in a FEM-technique which allows the load to be applied in one single step, only, even when the incremental theory of plastic flow has to be used.

Two self-similar problems are solved. Firstly an analytically solvable anti-plane strain crack problem is treated and the numerical one step solution is found to agree very well with the analytical one and significantly better than a step-by-step solution. Secondly a mode I crack problem for asymptotic small scale yielding in plane stress is examined. The result suggests that the plasticity correction for the crack length is significantly less than estimated by Tada et al. [1].

1. Introduction

When non-proportional loading is regarded, numerical solutions to elastic-plastic crack problems are usually obtained by applying the load in several increments. Therefore the accuracy of the result depends on the choices of these increments (i.e. the step size at different load levels) as well as on the accuracy of each incremental solution. However, in certain important cases this step-by-step solution can be avoided. These cases are characterized by self-similarity, at least approximately. This implies that the plastic stress-strain field remains essentially unchanged apart from a length scaling factor. When the plastic zone develops at the tip of a crack in a plate of ductile material, there is often a phase of approximate self-similarity at which the length scaling factor can be set to $(K/\sigma_Y)^2$ where K is the stress intensity factor and σ_Y is the yield stress.

2. Self-similarity

A stationary crack in a body subjected to monotonically increasing load is studied. It is assumed that the characteristic dimensions of the fracture process region are so small that this region can be regarded as a singular point. Further it is assumed that all characteristic in-plane dimensions of the plate, including the crack length, are much larger than the linear extension of the plastic zone and that the plate thickness is such that plane conditions can be assumed. Then, as the load is increased, the subsequent near-tip stress and strain states are self-similar, i.e. the only significant length parameter is $(K/\sigma_Y)^2$. In this case the total strain history can be traced along rays diverging radially out from the crack tip, i.e. on $\theta = \text{const.}$ in a polar coordinate system, see Fig. 1.

This has been taken advantage of in a finite element code operating according to the initial stress approach for non-linear problems as described by Nayak and Zienkiewicz [2].

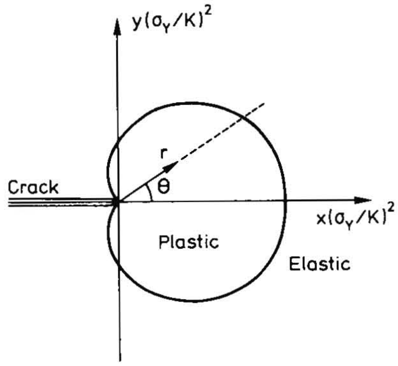

Figure 1. The strain history can be traced along rays diverging from $r = 0$.

8-node isoparametric elements are used throughout and element stiffnesses are integrated from 2 by 2 element integration points. Usually the stress $\sigma_{ij}(r, \theta)$ is determined by integration over the total strain history, from $\epsilon_{kl}(r, \theta) = 0$ before the load is applied, to the current strain $\epsilon_{kl}(r, \theta) = \epsilon^0_{kl}(r, \theta)$:

$$\sigma_{ij}(r, \theta) = \int_0^{\epsilon^0_{kl}(r,\theta)} D^{ep}_{ijkl} \, d\epsilon_{kl} \tag{1}$$

where D^{ep}_{ijkl} is the stress dependent elastic-plastic stress-strain matrix. Assuming, for a moment, self-similarity to be satisfied in the whole plane, then the integral in (1) can be converted to an integral over the distance r from the crack tip at a constant value of θ. Assuming further that the strain $\epsilon_{kl}(\infty, \theta) \to 0$ as $r \to \infty$, one obtains:

$$\sigma_{ij}(r, \theta) = \int_0^{\epsilon^0_{kl}(r,\theta)} D^{ep}_{ijkl} \, d\epsilon_{kl} = \int_\infty^r D^{ep}_{ijkl}(\partial\epsilon_{kl}/\partial r) \, dr. \tag{2}$$

Now integration according to (1) can be performed analytically for strains within the elastic region. This implies that numerical calculation of the integral in the right member of (2) need not be extended to infinity, but rather to a radius R large enough to reach the elastic region. Thus

$$\sigma_{ij}(r, \theta) = \sigma_{ij}(R, \theta) + \int_R^r D^{ep}_{ijkl}(\partial\epsilon_{kl}/\partial r) \, dr \tag{3}$$

where $\sigma_{ij}(R, \theta)$ is the analytically determined part. Obviously, relation (3) is correct even if self-similarity does not hold for the whole plane, but it must hold within the radius R.

The strain is found by linear interpolation between the element integration points r_n and r_{n+1} which must be situated at the same θ-coordinate (see Fig. 2), i.e.

$$\frac{\partial\epsilon_{kl}}{\partial r} = \frac{\epsilon_{kl}(r_{n+1}, \theta) - \epsilon_{kl}(r_n, \theta)}{r_{n+1} - r_n} = \text{const.} \quad \text{for } r_{n+1} \leqslant r \leqslant r_n. \tag{4}$$

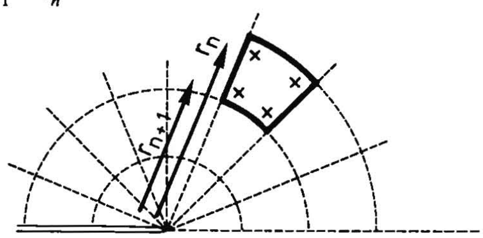

Figure 2. The strain-state is linearized between the integration points at $r = r_n$ and $r = r_{n+1}$ on a ray $\theta = \text{const.}$

By choosing, for simplicity, to calculate the stress first at r_n and then at r_{n+1} we arrive at the recursive relation

$$\sigma_{ij}(r_{n+1}, \theta) = \sigma_{ij}(r_n, \theta) + \frac{\epsilon^0_{kl}(r_{n+1}, \theta) - \epsilon^0_{kl}(r_n, \theta)}{r_{n+1} - r_n} \int_{r_n}^{r_{n+1}} D^{ep}_{ijkl} \, \mathrm{d}r \tag{5}$$

where the integral is calculated analytically as long as r_n and r_{n+1} are situated within the elastic region. Iterations are performed as described by [2], after replacing (1) with (5). After starting with a suitable assumption about the displacement field (for instance the elastic field), the deviations from the correct solution manifest themselves by non-zero resultant nodal forces. From these forces a corrective set of displacements is calculated, making use of the matrix of compliance. The procedure is greatly simplified by the fact that this matrix need not be updated in each loop, but the one for the linearly elastic material can be used instead. Actually there does not seem to be any advantage of updating the matrix at all in the two present cases. The iterations are repeated until the residual nodal forces are sufficiently small (cf. [2] for a detailed description).

3. A mode III elastic-plastic crack problem

The mode III elastic-perfectly-plastic small scale yielding problem solved analytically by Hult and McClintock [3] is chosen for demonstration. In the present numerical treatment the upper part, $0 \leqslant \theta \leqslant \pi$, of an infinitely long cylinder, $r \leqslant a$, with a crack in the plane $\theta = 0$, and the crack edge at $r = 0$ is studied (see Fig. 3). The cylinder cross-section is covered by 64 8-node isoparametric elements. The analytical solution [3] is used to specify the boundary conditions on the mantle surface. One obtains

$$\tau_{\theta z} = 0 \qquad \text{on} \quad \theta = \pi \tag{6}$$

and

$$\tau_{rz} = K_{III}\{2\pi r_0\}^{-1/2}[-\cos\theta \sin(\theta_0/2) + \sin\theta \cos(\theta_0/2)] \tag{7}$$

on

$$r = a, \quad 0 \leqslant \theta \leqslant \pi$$

where $r_0 = [(x - x_0)^2 + y^2]^{1/2}$, $\theta_0 = \tan^{-1}[y/(x - x_0)]$ and $x_0 = (3/2\pi)(\mathrm{K_{III}}/\sigma_\mathrm{Y})^2$. The choice $K_{III} = \sigma_Y(0.8a)^{1/2}$ is made. The remaining boundary condition is

$$w = 0 \qquad \text{on} \quad \theta = 0. \tag{8}$$

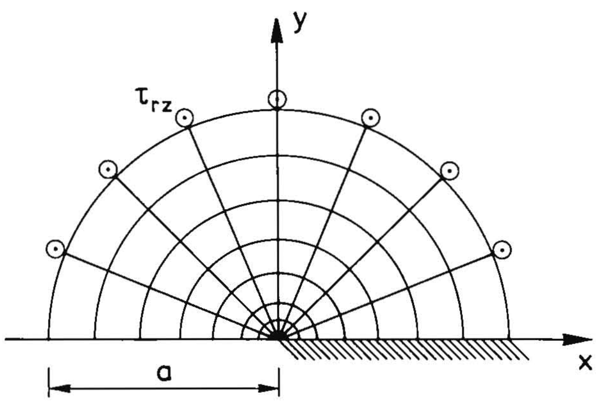

Figure 3. Cross-section of the cylinder considered in the FEM-calculations showing the mesh used.

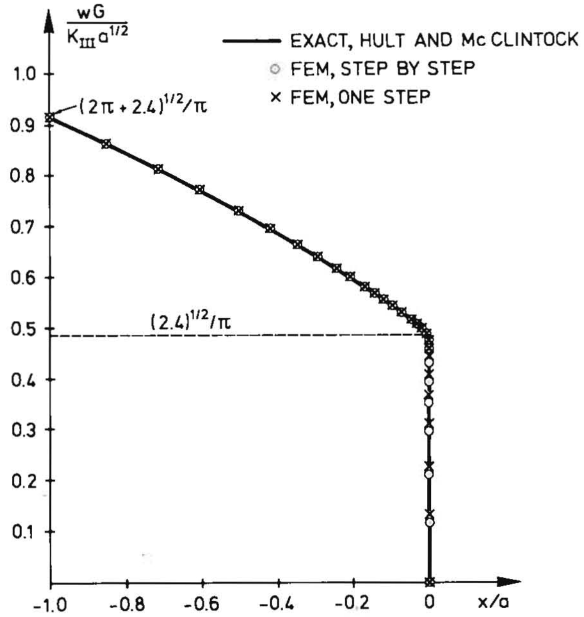

Figure 4. The non-dimensional displacement $wG/(K_{III}a^{1/2})$ versus the non-dimensional distance x/a along $y = 0$. At $x = 0$, the crack tip, the displacement is multi-valued, but can be specified by the angle from which $x = 0$ is approached (see Fig. 5).

The crack tip elements are degenerated to triangles, thus allowing an r^{-1} type of strain singularity at the crack tip, c.f. [3] and [4]. The elastic displacement field is first calculated and used as starter field. In the first iterations perfect plasticity cannot be introduced because of stability problems. Therefore a linearly hardening material with tangent modulus $E_t = E/10$ was assumed for the first iterations, whereupon perfect plasticity ($E_t = 0$) was introduced. The total number of iterations was 17. More iterations did not

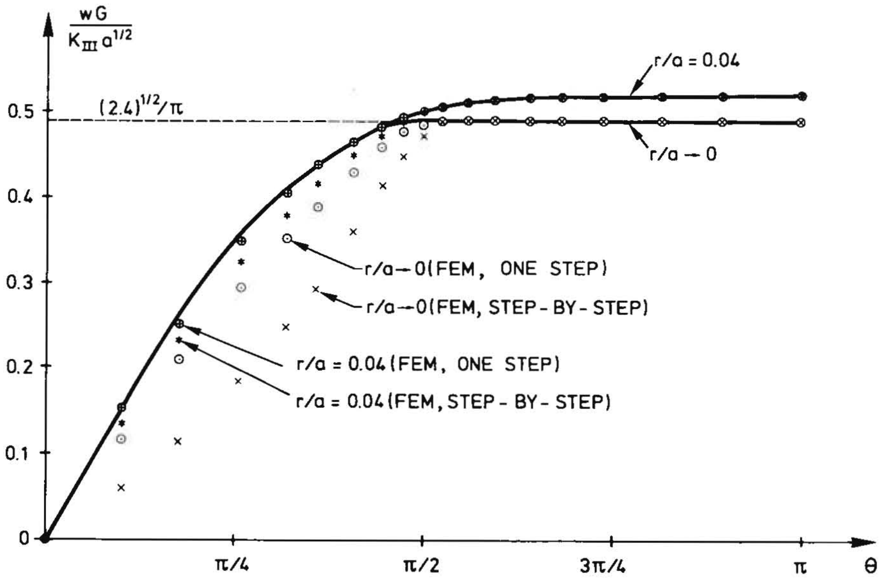

Figure 5. The non-dimensional displacement $wG/(K_{III}a^{1/2})$ versus the angle θ at the non-dimensional distances from the crack tip $r/a = 0.04$ and $r/a \to 0$.

improve the result. Figures 4 and 5 show displacements obtained at different points and the same displacements obtained both analytically (the exact result) and with an incremental (step-by-step) technique. For the step-by-step method (1) is used instead of (5) in the iteration loop described previously. Both numerical solutions are observed to agree well with the analytical solution but the one step solution givės the most accurate results, especially at the crack tip.

In the example chosen proportional loading prevails. However, this fact is neither required nor taken advantage of in the one step solution.

4. Plasticity correction of mode I crack lengths

At small scale yielding there is an annular region A around the crack tip in which the stress field closely coincides with the field given by the square root singular stress terms in the Williams expansion [5] around $x = 0$, $y = 0$ (the crack tip). The square root singular terms of the stress components (σ_x, σ_y, etc.) determine together a unique associated displacement field.

The elastic-plastic near-tip field can be found by studying a circular region (with radius R) around the crack tip, using the singular stress field for boundary conditions. If this region extends beyond the annular region A, second order regular terms in the Williams expansion cannot be neglected. On the other hand, if it does not reach this annular region, second-order singular terms (r^{-1}, $r^{-3/2}$, etc.) must be considered.

At (infinitesimally) small scale yielding the inner radius of the annular region A in which second-order terms can be neglected is much larger than the linear extension of the plastic region. Ideally then, the radius R should be larger than this inner radius. However, this condition might be difficult to satisfy when finite element methods are used. Therefore, in the following, R is assumed to be smaller than the inner radius of the annular region A and thus second (and higher) order singular terms become significant.

How would one know anything about the influence of second order stress terms? One way would be to study the boundary displacements at $r = R$ found after using the square root singular stress field for boundary conditions. If R actually was situated inside the annular region A these displacements would agree with those associated with the square root singular stress field. By checking this agreement a judgement can be made about the influence of neglecting second order boundary stress terms.

A possibility to improve the accuracy is to add singular stress terms to the boundary conditions. This can be done simply by assuming the centre of a square root singular stress field to be situated, say, at $x = x_*$, $y = 0$ rather than at $x = y = 0$. Each component in this field should possess the same angular distribution as obtained from the Williams expansion. Assuming mode I and using a polar coordinate system r, θ with $r = 0$ at the crack tip and $\theta = \pm\pi$ along the crack surfaces one can calculate the stress components σ_r and $\tau_{r\theta}$ of this field at $r = R$. These components can be used as boundary conditions for the region $r \leqslant R$ together with the condition of traction free crack surfaces.

The elastic plastic problem can be solved numerically and the displacements u_r^n and u_θ^n at $r = R$ can be determined (n = numerical). These displacements will in general be different from u_r^a and u_θ^a obtained from the displacement field associated to the square root singular stress field (a = analytical). The differences, $\delta u_r = u_r^a - \alpha u_r^n$ and $\delta u_\theta = u_\theta^a - \alpha u_\theta^n$, where α is some numerical factor, vary with θ. By a sutable choice of α and x_* these differences can be made small, preferably by seeking the values of α and $x_* = x_0$ that minimize the integral

$$I = \int_0^{\pi} \left(\delta u_\theta^2 + \delta u_r^2\right) \mathrm{d}\theta. \qquad (9)$$

The reason why α is introduced instead of unity is that numerically and analytically calculated displacements are not quite comparable – in the present case the magnitude of the numerically calculated displacements suffer from a systematic error that makes them somewhat underestimated. Thus α turns out to be slightly larger than unity (about 1.01).

The minimization is first done analytically with respect to α and then, simply by trial and error, with respect to x_*. After x_0 has been found the result can be interpreted in the following way:

Assume that the crack tip is situated at $x = x_0$, $y = 0$ and that the material is linearly elastic. The stress field at some distance from the crack tip is then square root singular with respect to this point. This field equals approximately the real stress field not only in the annular region, where a square root singular stress field centered at the crack tip ($x = 0$, $y = 0$) is a good approximation, but also at the radius $r = R$ (and of course, in the whole intermediate region). Knowledge of x_0 therefore gives a possibility to compute the near-tip field at small scale yielding by regarding a fairly small region around the crack tip, only.

Another advantage is that the stress intensity factor K can be calculated more accurately by using formulas from the linear elastic fracture mechanics after adding x_0 to the crack length. Hence, the length x_0 can be identified with the so called plasticity correction introduced by Irwin and Paris [6].

A thin infinite plate of an elastic-perfectly-plastic material is now studied. For symmetry reasons only the upper half of the circular region $r \leqslant R$, $0 \leqslant \theta \leqslant \pi$ is studied. The boundary load is given by the components σ_r and $\tau_{r\theta}$ found from the singular stress terms in a Williams expansion around $x = x_*$, $y = 0$. After some calculations one obtains:

$$\sigma_\theta = 0 \quad \text{on} \quad \theta = \pi \tag{10}$$

and

$$\sigma_r = K(2\pi r_*)^{-1/2}\{1 - \sin(\theta_*/2) \times [\sin(3\theta_*/2)\cos(2\theta) - \cos(3\theta_*/2)\sin(2\theta)]\}\cos(\theta_*/2) \tag{11}$$

$$\tau_{r\theta} = K(2\pi r_*)^{-1/2}[\sin(3\theta_*/2)\sin(2\theta) + \cos(3\theta_*/2)\cos(2\theta)]\sin\theta_*/2 \tag{12}$$

on $r = R$, $0 \leqslant \theta \leqslant \pi$ where $r_* = [(x - x_*)^2 + y^2]^{1/2}$, $\theta_* = \tan^{-1}[y/(x - x_*)]$.

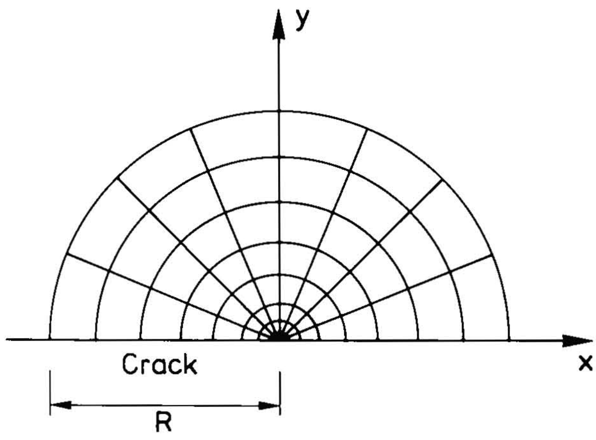

Figure 6. The element mesh used in the mode I case.

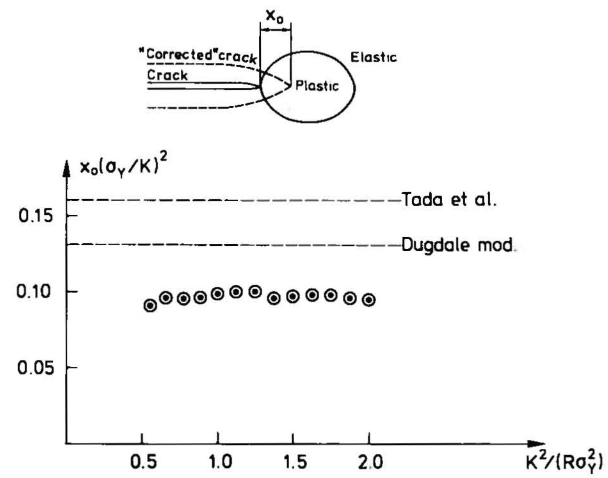

Figure 7. Non-dimensional plasticity correction $x_0(\sigma_Y/K)^2$ versus squared non-dimensional stress intensity factor $K^2/(R\sigma_Y^2)$. The corrections suggested by Tada et al. [1] and by Edmunds and Willis [8] are also indicated.

Furthermore the displacement in the y-direction

$$v = 0 \quad \text{on} \quad \theta = 0. \tag{13}$$

The half-circular region is covered by 64 8-node isoparametric elements (see Fig. 6) and self-similarity is taken advantage of to obtain a solution in one step as previously explained.

The investigation was carried out for values of K giving plastic zone sizes ranging from $R/8$ to $R/2$. The estimated value of x_0 is shown in Fig. 7. The result suggests a significantly smaller correction than what is recommended by Tada et al. [1]. A somewhat better agreement is found if the result is compared with the Dugdale model [7], for which $x_0 = (\pi/24)(K/\sigma_Y)^2 \approx 0.131(K/\sigma_Y)^2$ provides an asymptotic correction, according to analytical results by Edmunds and Willis [8].

The size of the plastic zone is observed to be slightly less than what is estimated by [1] and [8] (see Fig. 8). The scatter is due to the fact that the plastic zone size can be determined only within an error equal to the radial distance between integration points, as an inspection of Fig. 9 reveals.

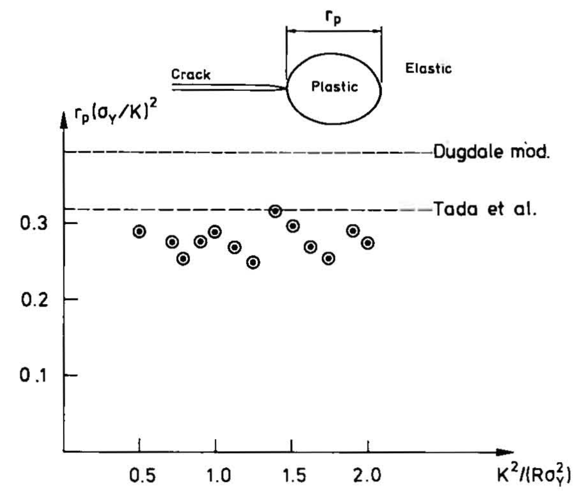

Figure 8. Non-dimensional plastic zone length $r_p(\sigma_Y/K)^2$ versus $K^2/(R\sigma_Y^2)$. The result obtained by Tada et al. [1] and the result for the Dugdale model [7] are also indicated.

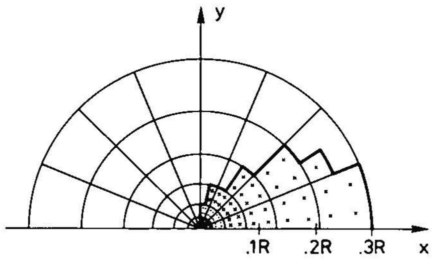

Figure 9. A typical plastic zone shape found by the FEM technique used, here for $K = \sigma_Y R^{1/2}$.

5. Conclusions

Apart from being more accurate and more economical, the one step solution technique for self-similarity problems present several advantages compared to a step-by-step technique. Since the history dependence is eliminated, a solution can be obtained by iterations from any fairly reasonable solution. This opens a possibility to study the effect of slightly changed material parameters (E, ν, σ_Y, etc.) simply by continuing iterations after change of parameters, while it is necessary to start calculations anew from zero load at the step-by-step method.

Acknowledgement

The author would like to thank Professor K.B. Broberg for invaluable discussions and for critical comments on the manuscript.

References

[1] H. Tada, P. Paris and G. Irwin, *The Stress Analysis of Cracks Handbook*, Del Research Corp., Hellertown (1973).
[2] G.C. Nayak and O.C. Zienkiewicz, *International Journal of Numerical Methods in Engineering* 5 (1972) 113–135.
[3] J.A. Hult and F.A. McClintock, *Proceedings of the 9th International Congress of Applied Mechanics, Brussels* 8 (1956) 51–58.
[4] N. Levy, P.V. Marcal, W.J. Ostergren and J.R. Rice, *International Journal of Fracture Mechanics* 7 (1967) 143–156.
[5] M.L. Williams, *Journal of Applied Mechanics* 24 (1957) 109–114.
[6] G. Irwin and P. Paris, *Proceedings of the 7th Sagamore Ordinance Materials Research Conference* Syracuse University Press, Syracuse, New York (1961).
[7] D.S. Dugdale, *Journal of the Mechanics and Physics of Solids* 8 (1960) 100–104.
[8] T.M. Edmunds and J.R. Willis, *Journal of the Mechanics and Physics of Solids* 25 (1977) 423–455.

Résumé

Dans les problèmes d'auto-similitude, l'histoire des déformations est contenue dans et déductible depuis le champ de déformation à chaque étape du processus de mise en charge. On utilise cette particularité dans la technique d'analyse par éléments finis, qui permet d'appliquer une charge en une seule étape seulement, même s'il faut appliquer la théorie de l'écoulement plastique sous condition incrémentielle. On résoud deux problèmes d'auto-similitude. En l'occurence, on traite d'abord d'un problème de fissuration sous déformation anti-planaire, solutionable par voie analytique; la solution numérique en une étape que l'on trouve est en très bon accord avec la solution analytique, et est significativement meilleure que la solution par étapes successives. En second lieu, on examine un problème de fissure sous un mode I correspondant à un écoulement plastique à petite échelle en état plan de tension. Le résultat obtenu suggère que la correction de plasticité à appliquer pour tenir compte de la longueur de la fissure est sensiblement moindre que celle estimée par Tada et al. (Réf. 1).